Available online at www.sciencedirect.com

ScienceDirect

Mendeleev Commun., 2024, **34**, 854–858

Mendeleev Communications

Halonal, an original benzoylated phenobarbital derivative anticonvulsant: *in vivo* evaluation, chemometric and molecular docking studies of enantiomers

Tamara V. Shushpanova,*[a,b] Nikolay A. Bokhan,[a,c] Galina B. Slepchenko,[d] Evgeniya V. Markova,[e] Olga V. Shushpanova,[f] Irina N. Smirnova,[b] Alexei A. Zaitsev,[b] Natalia E. Kolomiets,[c,g] Vera Yu. Kuksenok[d] and Victor D. Filimonov[d]

[a] *Mental Health Research Institute, Tomsk National Research Medical Center, Russian Academy of Sciences, 634050 Tomsk, Russian Federation. E-mail: shush59@mail.ru*
[b] *Tomsk Research Institute of Balneology and Physiotherapy, Federal Scientific and Clinical Center for Medical Rehabilitation and Balneology, 634009 Tomsk, Russian Federation*
[c] *Siberian State Medical University, 634050 Tomsk, Russian Federation*
[d] *National Research Tomsk Polytechnic University, 634050 Tomsk, Russian Federation*
[e] *Research Institute of Fundamental and Clinical Immunology, 630099 Novosibirsk, Russian Federation*
[f] *Scientific Center of Mental Health, 115522 Moscow, Russian Federation*
[g] *Kemerovo State Medical University, 650056 Kemerovo, Russian Federation*

DOI: 10.1016/j.mencom.2024.10.027

An original phenobarbital anticonvulsant Halonal, 5-ethyl-1-(2-fluorobenzoyl)-5-phenylpyrimidine-2,4,6(1*H*,3*H*,5*H*)-trione, stimulated the cellular immune and the humoral response in long-term alcoholized male (CBAxC57Bl/6) F1 mice to the level of healthy animals. Voltammetry was found to be suitable for determination of Halonal *R*/*S*-enantiomeric ratio, which was exemplified on the authentic sample with the *R*/*S*-composition of 40 : 60. Molecular docking (Schrödinger program, Glide) showed that Halonal behaved as a benzonal derivative interacting with $GABA_AR$ *via* the BARB binding site, with *S*-Halonal having higher similarity score than its *R*-enantiomer because of a different orientation of the 2-fluorobenzoyl substituent.

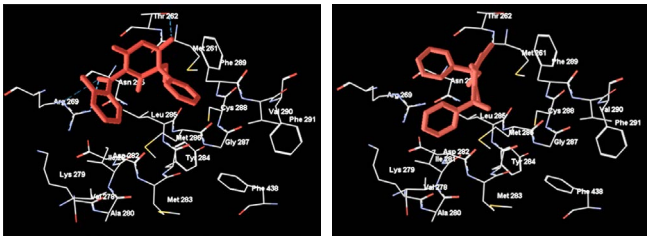

Keywords: anticonvulsant, γ-aminobutyric acid, molecular docking, $GABA_A$ receptor, enantiomer, barbiturates, 2-fluorobenzoyl substituent.

The introduction of new drugs into medical practice for the treatment of primarily socially significant diseases (including orphan diseases) is one of the priority tasks of healthcare. Various neurodegenerative, mental and addictive disorders are associated with $GABA_AR$ neuroplasticity in their development.[1–4] Barbiturate derivatives phenobarbital and barbital recommended to use as anticonvulsants, hypnotics, and for premedication, have a pronounced effect due to interaction with the barbiturate site of the GABA-C1-ionophore complex. However, the presence of adverse side effects in phenobarbital requires the search for new, safe drugs with neuroprotective and neuroimmune actions.

Halonal, 5-ethyl-1-(2-fluorobenzoyl)-5-phenylpyrimidine-2,4,6(1*H*,3*H*,5*H*)-trione is a derivative of barbituric acid. It is an anticonvulsant drug developed for the treatment of epilepsy, paroxysmal, addictive disorders and others.[5,6] On the other hand, the direction of our research has a targeted vector on the effectiveness of Halonal in the treatment and prevention of alcohol addiction.

The molecular modeling (molecular docking) method allows one to evaluate the geometry of ligand–receptor interactions of new chemical compounds based on their mechanism of action and the structure of the target being studied using computational platforms in combination with molecular and quantum mechanics. The crystal structure of the $GABA_AR$ α1β2γ2 heteropentamer is a receptor model optimized for studying interactions with agonists and allosteric modulators that bind to targets, *i.e.*, $GABA_AR$ sites of the multireceptor complex.[7,8] The pharmacological activity of the developed drug compounds is largely determined by the stereospecificity of its action and depends on the degree of compliance of its structure with the target receptor and enantiomeric purity.[7,8]

Halonal is an *N*-acylated phenobarbital derivative that does not cause a side hypnotic effect, which is due to the presence of an 2-fluorobenzoyl group in its structure. The presence of fluorine in the *ortho*-position in the *N*-benzoyl substituent

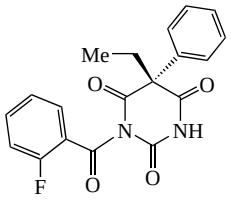

R-(–)-Halonal

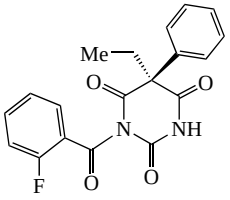

S-(+)-Halonal

reduces the toxicity of Halonal. Differences in the spatial structure of enantiomers determine their stereospecific binding to different receptor sites, and as a result can cause side effects in racemic drugs. The stereospecificity of the binding site of the enantiomeric forms of Halonal can provide differences in the characteristics of their binding to the GABA receptor and different therapeutic efficacy. In this regard, it is important to study both enantiomeric forms of Halonal for the highest stereospecificity of the GABA receptor sites to reduce side effects when using the racemate of the drug.

5-Substituted phenobarbital derivatives contain an asymmetric carbon atom, hence they should exist as two optical isomers. Some of such enantiomers have been studied previously.[9] Halonal also contains 5-positioned chiral carbon atom. Apparently, its *R*- and *S*-enantiomers should differ in pharmacokinetic and pharmacodynamic characteristics and should have different biological effects. According to quantum calculations of specific rotation, the absolute configuration of (+)- and (–)-Halonal was determined to be *S* and *R*, respectively.[9]

In this work, we performed chemometric and molecular docking studies of Halonal enantiomers and their interactions with the $GABA_A$ receptor based on molecular modeling, to evaluate the most effective drug candidate compared to the racemate, especially to ensure the minimum severity of possible side effects. We found that Halonal at a concentration of 65 mg kg^{-1} per day decreased alcohol motivation in experimental mice.[10] Stimulation of motor and exploratory activities in the Open Field test were recorded compared to untreated mice. Total horizontal motor activity was 36.9 ± 8.7 and 71.1 ± 10.7, and total vertical activity was 1.3 ± 0.5 and 13.4 ± 1.4 before and after Halonal therapy in alcoholized male (CBA × C57Bl/6) F1 mice, respectively ($p < 0.01$). The obtained data indicate a decrease in the severity of depressive-like behavior formed during long-term alcoholization. It suggests that $GABA_AR$ ligand Halonal, similar to its effects on neuronal cells, may cause modulation of the functional activity of the T-lymphocytes, thereby influencing the intensity of the neuroimmune response, used as an extracerebral model.

After treatment of alcoholized mice with Halonal, it was found that the intensity of the immune response changed. The humoral response was assessed by the relative number of antibody-forming spleen cells/10^6 nucleated cells (AFC1) and absolute number of antibody-forming spleen cells cells (AFC2); the cellular immune response was assessed by the height of the delayed-type hypersensitivity reaction (DTHR). A significant suppression of the humoral and cellular immune response in mice was revealed after long-term alcoholization (Table 1, experimental group 1). After a course of Halonal administration in mice (experimental group 2), an increase in the humoral immune response assessed by absolute and relative numbers of antibody-forming spleen to a level characteristic of healthy animals in the control group was recorded in long-term alcoholized mice. A significant stimulation of the cellular immune response assessed by the DTHR was also noted (see Table 1).

Table 1 Intensity of the humoral and cellular immune response in long-term alcoholized (CBA × C57BL/6) F1 mice after course of Halonal administration.

Animal group [a]	Relative number of antibody-forming spleen cells/10^6 nucleated cells (AFC1)	Absolute number of antibody-forming spleen cells (AFC2)	Delayed-type hypersensitivity reaction (DTHR) (%)
Control group	362.78 ± 68.3	69515.4 ± 8678.6	77.2 ± 2.3
Experimental group 1	50.21 ± 11.4[b]	8926.2 ± 418.2[b]	32.1 ± 1.4[b]
Experimental group 2	342.3 ± 49.5	68711.3 ± 9136.8	79.1 ± 4.7

[a] Control group represents healthy mice. Experimental group 1 represents long-term alcoholized mice. Experimental group 2 represents long-term alcoholized mice after course of Halonal administration. Results are presented as M ± SD. [b] $p < 0.01$ relative to the corresponding indicator in the control group.

Halonal, similar to its effect on neuronal cells, modulates the functional activity of T-lymphocytes, affecting the intensity of the neuroimmune response used as an extracerebral model and may be applicable in the future for studies with prognostic purposes in patients with alcohol dependence.

Chemometric processing of voltammetric curves was used to estimate the content of enantiomeric forms in the substance of Halonal. Based on the voltammograms of the *S*- and *R*-forms of Halonal, a chemometric assessment of the experimental results was carried out using the MathCAD program.[11] With an increase in the content of the *S*-form in the mixture, a shift in the maximum potential to the anodic region was observed. It was found that the pattern had a linear nature, this parameter was used to estimate the composition of the enantiomeric mixture of Halonal.[12] We differentiated analytical signals of levorotatory (*R*) and dextrorotatory (*S*) forms of Halonal. Using a gold-graphite electrode (GGE), we determined the operating conditions that allowed us to obtain a difference in signals of these forms by 30 mV, which is insufficient for an unambiguous assessment of the type of enantiomer. When studying analytical signals of enantiomer mixtures in various ratios, it was found that with an increase in the content of the dextrorotatory form, a shift in the potentials of the peak maxima to the cathode region was observed. Since the values of the analytical signal potentials do not allow us to unambiguously differentiate the composition of the enantiomeric mixture, chemometric data processing was used. Recording voltammograms of Halonal enantiomers on a GGE electrode against the background of a borate buffer with a pH of 9.18 is shown in Figure 1.

When comparing the graphs (see Figure 1) a tendency to change the nature of the voltamperic curves is noticeable, which can be used to separate analytical signals. The main parameter may be the increase in the maximum of the current–voltage characteristic as the concentration of the second solution increases to 50%. Dependence of the maximum peak potential of Halonal on the content of the levorotatory form is shown in Figure 2.

Figure 3 shows the evaluation of the Halonal enantiomers ratio using chemometric processing of data on the slope line of the current–voltage characteristics for (*a*) different contents of enantiomeric forms and (*b*) residual curves of the current–voltage characteristics minus the slope lines. The slope lines are shown at the top for the percentage of the *R*-form in the mixture (0, 20 and 40%). Hence, there is a regular increase in the slopes

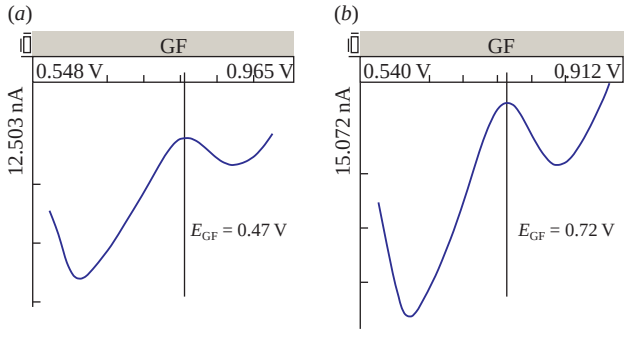

Figure 1 Parallel experiments on recording voltammograms of (*a*) (*R*)-(–)-Halonal and (*b*) (*S*)-(+)-Halonal on the GGE electrode against the background of a borate buffer with pH 9.18.

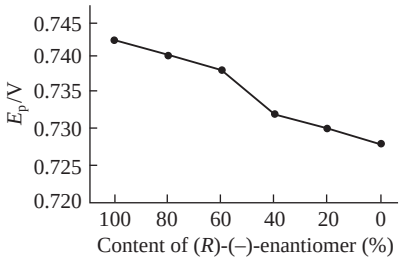

Figure 2 Dependence of the maximum peak potential of Halonal on the content of the (*R*)-(–)-form.

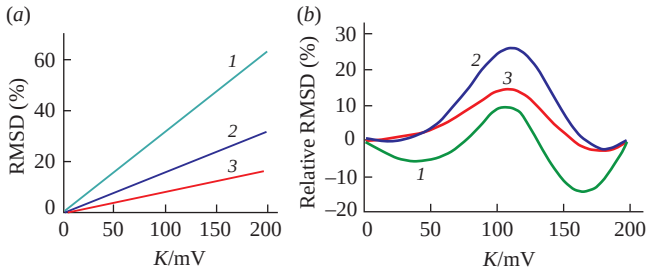

Figure 3 (*a*) Dependence of the root-mean-square deviations (RMSD) for (*S*)-(+)-Halonal in solution on the position of the maxima of their voltammetric characteristics. (*b*) Dependence of the relative RMSD for (*S*)-(+)-Halonal in solution on their voltammetric characteristics. Curves *1* stand for 0%, curves *2* for 20% and curves *3* for 40% of *R*-(–)-Halonal in the mixture, respectively. Parameter *K* stands for the positons of the maxima.

with increasing concentration. Values of the slope coefficients of the current–voltage characteristic curves (CVCC) depending on the content of the *R*-isomer in the mixture are presented in Table 2.

The concentration of *S*-Halonal is calculated from the *R*/*S* ratio, *i.e*. with 40% of the *R*-form the concentration of the *S*-form should be 60%. The slope coefficients are a good criterion for estimating the enantiomeric composition of a studied sample when using the interpolation procedure. Herein, experimental voltammetric study of the authentic sample having *R*/*S* ratio of 40 : 60 gave the correct value of 60% for the *S*-form in the mixture. Thus, the method for determining the ratio of Halonal enantiomers using voltammetry is developed. Model solutions of Halonal with different *R*/*S* ratios (0 : 100, 20 : 80 and 40 : 60) were prepared by mixing the solutions of the *R*- and *S*-enantiomers. Individual enantiomers of Halonal were obtained upon separation of the racemate using Agilent Ultron ES-OVM-C chiral chromatography column [mobile phase was the 1 : 9 MeCN–phosphate buffer (0.02 M, pH 4.4), isocratic elution]. Figure 3 shows the slope lines for Halonal solutions with different percentage of *R*-isomer in the mixture (0, 20, 40%). An increase in slopes with increasing of concentration is observed. Table 2 shows the values of the slope coefficients of the CVCC derived from the content of the *R*-enantiomer in the mixture. This approach allows one to evaluate the ratio of enantiomers, which is an important analytical task to ensure the sustainability of quality of each batch of the synthesized drug.

Table 2 Dependence of slope coefficients of CVCC on the enantiomeric composition of Halonal sample.

Content of (*R*)-(–)-form (%)	Slope coefficients of the *I*–*V* curves	Positions of the maxima/mV
0	0.083	110
20	0.161	108
40	0.317	106
60	0.341	96
80	0.431	94
100	0.455	90

For the docking studies, the previously[13] described unified model of the most abundant subtype of the $GABA_AR$ $\alpha_1\beta_2\gamma_2$ was used. Prior to docking, the model protein was preprocessed by protein preparation wizard in Maestro (Maestro, version 10.2, Schrödinger, LLC, New York, NY, 2015). Halonal was subjected to the ligand preparation by LigPrep (LigPrep, version 2.3, Schrödinger, LLC, New York, NY, 2009) with generation of possible protonation states using Epik (Epik, version 2.0, Schrödinger, LLC, New York, NY, 2009).[14] Ligands were docked into the box covering the benzodiazepine binding site (BZD) located at the $\alpha_1\gamma_2$ interface. Box had auto size and was centroid onto the Diazepam. Ligands were docked as flexible molecules. Docking was performed using Glide (Glide, version 6.7, Schrödinger, LLC, New York, NY, 2015) in Induced Fit Docking mode according to standard protocol with the use of Extra Precision scoring function. GlideScore scoring function was used for identification of the best-docked ligand pose.[15,16]

Since the $GABA_AR$ unified model was optimized for agonists and BZD allosteric modulators, we were unable to use it for docking into barbiturate binding site (BARB),[13] which, in addition, has not been precisely defined yet. The other available receptor crystal structure consists of β_3 subunits[17] and in this case it is also not suitable for docking since the BARB binding site, supposed to be located on $\alpha\beta_2$ or $\alpha\beta_3$ interface. However, there are many barbiturates with the known structure and activity, which are supposed to act as $GABA_AR$ positive allosteric modulators.

We docked in two regions: a 9 Å sphere encompassing the benzodiazepine site (based on the position of the ligand crystallized by the receptor) and a 9 Å sphere centered on the M286 coordinates (barbiturate site). The *R*- and *S*-Halonal isomers were used as the ligands. According to the calculation, none of the listed ligands were complementary to the benzodiazepine site (no energy gain upon binding): the Halonal molecule was not complementary to the benzodiazepine binding site. However, Halonal interacted with the barbiturate site of $GABA_A$ receptor by binding to M286 of the β2 subunit and M235 of the α1 subunit. The binding pocket itself is rather 'fuzzy' and Halonal, as a more 'bulky' molecule, is more complementary to it. At the same time, *R*-Halonal binds more effectively than its *S*-isomer. The *R*-isomer of Halonal geometrically fits well into the pocket formed by M286 at the interface of the β3 subunit, interacts significantly with M286, plus forms hydrogen bonds with Arg269 and Thr262 (Figure 4) marked with blue dashed-dotted lines). In the docking studies, Halonal was regarded as flexible molecule. It permitted to evaluate the binding energy of the ligand in various poses as well as the stability of obtained complexes. The determined best-docked ligand poses for *S*- and *R*-Halonal enantiomers were the most stable comparing to other poses.

Membrane permeability of Halonal was calculated using Physics-Based ADME/Tox tool in Maestro (Maestro, version 10.2, Schrödinger, LLC, New York, NY, 2015). Logarithm of membrane permeability (Log Perm.) of the RRCK (MDCK-LE) and the total free energy penalty for the ligand to change state the neutral form and enter the membrane (move from the high dielectric region to the low dielectric region) (dG_Insert) were calculated.

Despite the fact that no experimental crystal structure of $GABA_AR$ $\alpha_1\beta_2\gamma_2$ heteropentamer is available to date, a unified pharmacophore models summarizing the structure–activity (SAR) relationships of compounds acting as a BZD site allosteric modulators and mutational analysis data allowed for the precise positioning of Diazepam in BZD binding pocket.[13] BZD binding site is located on $\alpha_1\gamma_2$ interface of $GABA_AR$ and formed by α_1Tyr159, α_1Thr206, α_1Gly207, α_1Phe99, α_1Hid101,

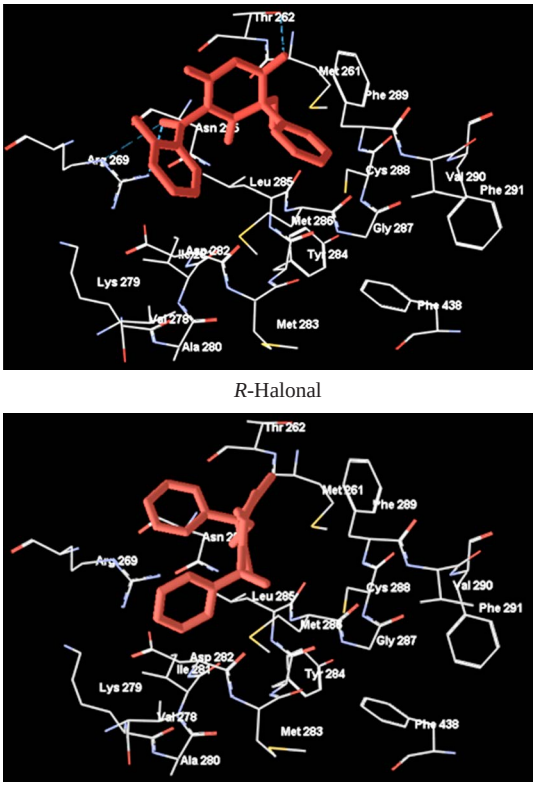

R-Halonal

S-Halonal

Figure 4 The binding modes of Halonal enantiomers in the BARB-binding pocket of $GABA_A$ receptor (α1β2γ2).

α_1Tyr209, and γ_2Phe77 residues. Residues α_1Gly200, α_1Val202, and γ_2Met130 line the binding pocket. Diazepam has a fused aromatic ring system, which is a lipophilic pharmacophoric feature supposed to be an essential part of benzodiazepins (BZDs).[18] This moiety is located in a BZD pocket beneath the C-loop and surrounded by the hydrophobic residues α_1Val202, α_1Tyr209, and α_1Val211. It is also involved in π–π stacking with α_1Tyr209.

The carbonyl moiety of Diazepam is also located under the C-loop and forms two hydrogen bonds with γ_2Thr142 and α_1Thr206 residues. The α_1Tyr209 and α_1Thr206 residues are strongly required for ligand binding in BZD site, which was previously demonstrated by the mutational analysis.[19,20] The phenyl ring of Diazepam is located in a hydrophobic box formed by α_1Phe99, α_1His101, α_1Tyr159, γ_2Phe77 and γ_2Asn128 and act as a strong link between α_1 and γ_2 subunits[13] [Figure 5(*a*),(*b*), Diazepam is shown in light blue].

A docking study conducted for Halonal enantiomers demonstrates that it binds to the receptor BZD pocket in very different fashion than Diazepam occupying the distal part of the binding site. It may be explained by the fact that large Halonal molecule cannot penetrate to the narrow hydrophobic pocket of the BZD site as Diazepam. Despite the fact that the carbonyl moieties of barbiturate core of both enantiomers form a hydrogen bond with α_1Thr206 and α_1Tyr209, a hydrophobic box formed by α_1Phe99, α_1Hid101, α_1Tyr159, γ_2Phe77 and γ_2Asn128 is left empty. It was previously demonstrated that positive BZD modulators trigger specific conformational changes of $GABA_AR$; moreover, modulation of I_{GABA} by different BZDs requires specific residues in Loop F.[21,22] Thus, such a big difference in geometry and interaction with the binding pocket between the Halonal and Diazepam allows us to suggest that Halonal does not act as a BZD site allosteric modulator since it might cause inappropriate conformational changes of the receptor.

To assess RRCK (MDCK-LE) membrane permeability of Halonal, the ADME/Tox calculations were performed. Membrane permeability slightly differs between enantiomers, which might be caused by different energy penalty for tautomerization. Halonal is characterized by absorption potential ($<2.5\times10^{-6}$ cm s^{-1}).[23] This is in compliance with calculated total free energy penalty for the ligand to enter the membrane: for Halonal it is two times higher. According to the empirical SAR analysis performed for barbiturates, 5-positioned alkyl and

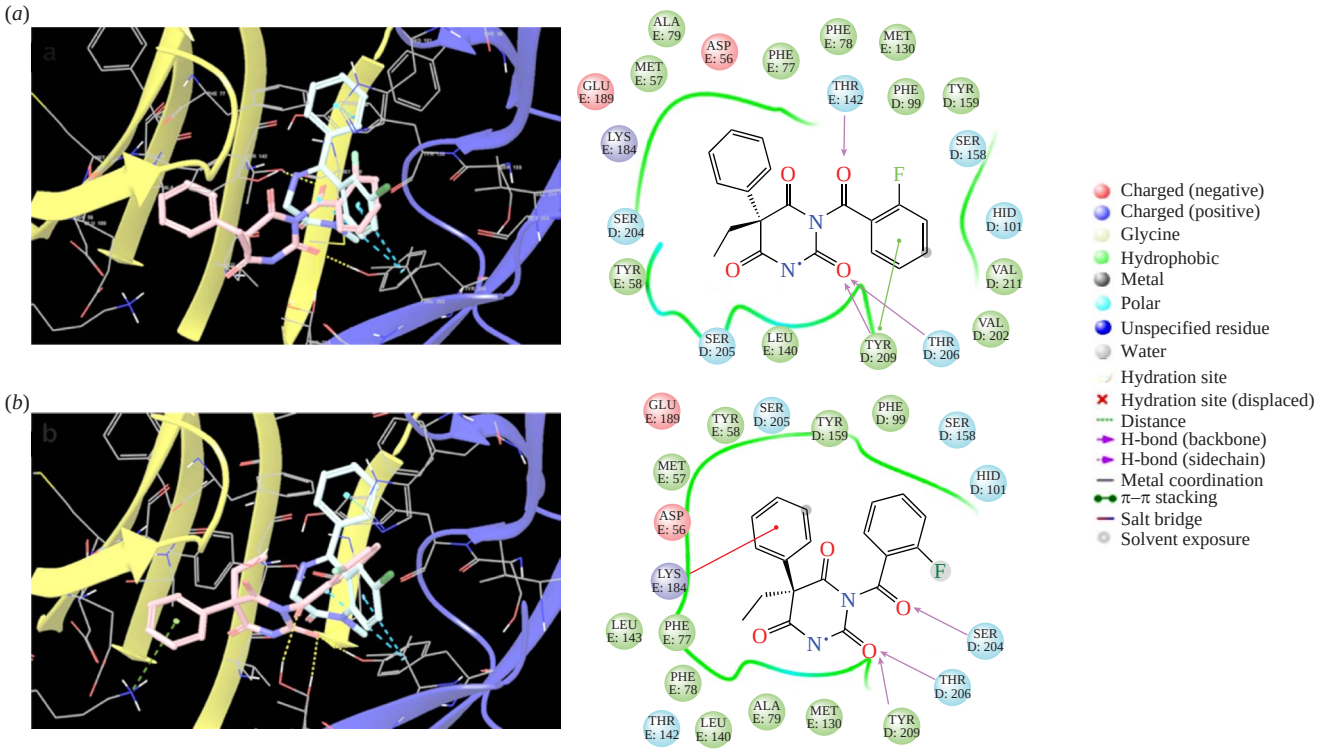

Figure 5 The position of Halonal (visualized in pink) in the benzodiazepine binding site of $GABA_AR$ overlapped with Diazepam (visualized in light blue) and 2D map reflecting the interaction of the Halonal with the residues in the binding pocket (D – α_1, E – γ_2): (*a*) *R*-Halonal (GScore is –11.1 kcal mol^{-1}); (*b*) *S*-Halonal (GScore is –11.8 kcal mol^{-1}).

Table 3 Summary of the Halonal interaction with $GABA_AR$.

Ligand	Log Perm.[a]	Perm. /cm s^{-1}	d*G* Insert[b]	GScore (BZD pocket)	Similarity (BARB pocket)
R-Halonal	–5.844	1.4×10^{-6}	13.33	–11.1	0.717
S-Halonal	–5.849	1.4×10^{-6}	13.47	–11.8	0.792

[a] Calculated logarithm of membrane permeability of the RRCK (MDCK-LE). [b] The total free energy penalty for the ligand to enter the membrane (move from the high dielectric region to the low dielectric region).

aromatic substituents cause lower lipid solubility and lower activity of the compound, at the same time decreasing its hypnotic activity and making it long-acting.[24] This might explain low absorption potential calculated for Halonal.

Taking into account that Halonal has a barbiturate scaffold and is a derivative of Benzonal it could be proposed that it interacts with the $GABA_AR$ through the BARB binding site. However, it could be noticed that *S*-Halonal is characterized by a higher measure of similarity (Table 3) since it fully overlaps the template, whereas *R*-Halonal has a different orientation of 2-fluorobenzoyl substituent situated beyond the model. It has been shown that acylation of barbiturates at the N^1 position reduces sedative effects; Halonal is a phenobarbital acylated with 2-fluorobenzoic acid at the N^1 position, which is more advantageous than phenobarbital when used as an anticonvulsant.

Creation of innovative anticonvulsants that modulate the activity of the $GABA_A$ receptor and do not have pronounced sedative effects is promising in the treatment of socially significant diseases, and, first of all, neurological, mental and addictive disorders associated with $GABA_AR$ neuroplasticity in their development.[25]

The results we obtained during the study allow us to recommend further research of the original anticonvulsant Halonal in the treatment of alcohol dependence as one of the modern pharmacotherapeutic agents. The development of new domestic drugs aimed at creating etiopathogenetic therapy for patients suffering from addiction diseases and alcohol dependence not causing adverse reactions (mental sedation and others) makes it possible to increase the effectiveness of the therapy and reduce the cost of treatment.

The study was carried out at the expense of budget financing under the main plan of research for 2022–2026 ‘A multi-disciplinary study of clinical heterogeneity and pathobiological mechanisms of the progressive development of addictive disorders with the development of innovative therapy programs and differentiated prevention’ (State registration no. 122020200053-1).

Online Supplementary Materials

Supplementary data associated with this article can be found in the online version at doi: 10.1016/j.mencom.2024.10.027.

References

1 S. De Santis, A. Cosa-Linan, R. Garcia-Hernandez, L. Dmytrenko, L. Vargova, I. Vorisek, S. Stopponi, P. Bach, P. Kirsch, F. Kiefer, R. Ciccocioppo, E. Sykova, D. Moratal, W. H. Sommer and S. Canals, *Sci. Adv.*, 2020, **6**, eaba0154; https://doi.org/10.1126/sciadv.aba0154.
2 G. F. Koob and N. D. Volkow, *The Lancet Psychiatry*, 2016, **3**, 760; https://doi.org/10.1016/S2215-0366(16)00104-8.
3 R. W. Olsen and J. Liang, *Mol. Brain*, 2017, **10**, Article 45; https://doi.org/10.1186/s13041-017-0325-8.
4 T. V. Shushpanova, N. A. Bokhan, V. F. Lebedeva, A. V. Solonskii and V. V. Udut, *J. Psychiatry*, 2016, **19**, 1000365; https://doi.org/10.4172/2378-5756.1000365.
5 M. Bialer, *Epilepsia*, 2012, **53**, 26; https://doi.org/10.1111/j.1528-1167.2012.03712.x.
6 T. P. Novozheyeva, M. I. Smagina, N. A. Cherevko and S. N. Fateyeva, *Byulleten Sibirskoi Meditsiny*, 2011, **10** (5), 78 (in Russian); https://doi.org/10.20538/1682-0363-2011-5-78-81.
7 M. J. Amundarain, J. F Viso, F. Zamarreño, A. Giorgetti and M. Costabel, *J. Biomol. Struct. Dyn.*, 2019, **37**, 1597; https://doi.org/10.1080/07391102.2018.1462733.
8 M. J. Amundarain, R. P. Ribeiro, M. D. Costabel and A. Giorgetti, *Future Med. Chem.*, 2019, **11**, 229; https://doi.org/10.4155/fmc-2018-0336.
9 A. Ceccato, B. Boulanger, P. Chiap, Ph. Hubert and J. Crommen, *J. Chromatogr.*, 1998, **819**, 143; https://doi.org/10.1016/S0021-9673(98)00547-0.
10 E. Markova, I. Savkin, M. Knyazheva and T. Shushpanova, *Eur. Psychiatry*, 2021, **64**, S821; https://doi.org/10.1192/j.eurpsy.2021.2171.
11 V. Mirceski, R. Gulaboski and I. Kuzmanovski, *Bull. Chem. Technol. Maced.*, 1999, **18** (1), 57; https://repository.ukim.mk/bitstream/20.500.12188/12986/1/XIII_0909.pdf.
12 O. Mezentseva, G. Slepchenko, V. Filimonov, E. Mikheeva and G. Arbit, *Electroanalysis*, 2019, **31**, 1477; https://doi.org/10.1002/elan.201900179.
13 R. Bergmann, K. Kongsbak, P. L. Sørensen, T. Sander and Th. Balle, *PLoS One*, 2013, **8**, e52323; https://doi.org/10.1371/journal.pone.0052323.
14 G. Madhavi Sastry, M. Adzhigirey, T. Day, R. Annabhimoju and W. Sherman, *J. Comput.-Aided Mol. Des.*, 2013, **27**, 221; https://doi.org/10.1007/s10822-013-9644-8.
15 T. A. Halgren, R. B. Murphy, R. A. Friesner, H. S. Beard, L. L. Frye, W. T. Pollard and J. L. Banks, *J. Med. Chem.*, 2004, **47**, 1750; https://doi.org/10.1021/jm030644s.
16 R. A. Friesner, R. B. Murphy, M. P. Repasky, L. L. Frye, J. R. Greenwood, T. A. Halgren, P. C. Sanschagrin and D. T. Mainz, *J. Med. Chem.*, 2006, **49**, 6177; https://doi.org/10.1021/jm051256o.
17 P. S. Miller and A. R. Aricescu, *Nature*, 2014, **512**, 270; https://doi.org/10.1038/nature13293.
18 W. Zhang, K. F. Koehler, P. Zhang and J. M. Cook, *Drug Des. Discov.*, 1995, **12**, 193; https://pubmed.ncbi.nlm.nih.gov/7662830.
19 K. R. Tan, R. Baur, S. Charon, M. Goeldner and E. Sigel, *J. Neurochem.*, 2009, **111**, 1264; https://doi.org/10.1111/j.1471-4159.2009.06419.x.
20 A. Buhr, M. T. Schaerer, R. Baur and E. Sigel, *Mol. Pharmacol.*, 1997, **52**, 676; https://doi.org/10.1124/mol.52.4.676.
21 S. M. Hanson and C. Czajkowski, *J. Neurosci.*, 2008, **28**, 3490; https://doi.org/10.1523/JNEUROSCI.5727-07.2008.
22 N. C. Pflanz, A. W. Daszkowski, G. L. Cornelison, J. R. Trudell and S. J. Mihic, *J. Biol. Chem.*, 2018, **293**, 8264; https://doi.org/10.1074/jbc.RA118.002128.
23 L. Di, C. Whitney-Pickett, J. P. Umland, H. Zhang, X. Zhang, D. F. Gebhard, Y. Lai, J. J. Federico, R. E. Davidson, R. Smith, E. L. Reyner, C. Lee, B. Feng, C. Rotter, M. V. Varma, S. Kempshall, K. Fenner, A. F. El-Kattan, T. E. Liston and M. D. Troutman, *J. Pharm. Sci.*, 2011, **100**, 4974; https://doi.org/10.1002/jps.22674.
24 A. Gringauz, *Introduction to Medicinal Chemistry: How Drugs Act and Why*, Wiley-VCH, New York, 1997; https://www.wiley.com/en-us/Introduction+to+Medicinal+Chemistry%3A+How+Drugs+Act+and+Why-p-9780471185451.
25 T. V. Shushpanova, N. A. Bokhan, K. S. Stankevich, T. P. Novozheeva, A. I. Mandel, E. D. Schastnyi, N. I. Kisel, O. V. Shushpanova, V. V. Udut, S. M. Safronov, R. S. Boev and E. M. Knyazeva, *Pharm. Chem. J.*, 2021, **54**, 1093; https://doi.org/10.1007/s11094-021-02327-x.

Received: 27th June 2024; Com. 24/7561